

## ***In vivo* evaluation of corneal biomechanical properties by optical coherence elastography at different cross-linking irradiances**

Yuheng Zhou  
Yuanyuan Wang  
Meixiao Shen  
Zi Jin  
Yihong Chen  
Yue Zhou  
Jia Qu  
Dexi Zhu

# *In vivo* evaluation of corneal biomechanical properties by optical coherence elastography at different cross-linking irradiances

Yuheng Zhou, Yuanyuan Wang, Meixiao Shen, Zi Jin, Yihong Chen, Yue Zhou, Jia Qu, and Dexi Zhu\*  
Wenzhou Medical University, School of Ophthalmology and Optometry, Wenzhou, China

**Abstract.** Corneal collagen cross-linking (CXL) strengthens the biomechanical properties of damaged corneas. Quantifying the changes of stiffness due to different CXL protocols is difficult, especially *in vivo*. A noninvasive elastic wave-based optical coherence elastography system was developed to construct *in vivo* corneal elasticity maps by excitation of air puff. Biomechanical differences were compared for rabbit corneas given three different CXL protocols while keeping the total energy delivered constant. The Young's modulus was weaker in corneas treated with higher irradiance levels over shorter durations, and a slight increase of Young's modulus was present in all groups one week after the recovery process. Due to the noninvasive nature and minimal force to generate corneal elastic waves, this technique has the potential for early detection and treatment of corneal diseases in clinic. © The Authors. Published by SPIE under a Creative Commons Attribution 4.0 Unported License. Distribution or reproduction of this work in whole or in part requires full attribution of the original publication, including its DOI. [DOI: 10.1117/1.JBO.24.10.105001]

Keywords: optical coherence elastography; collagen cross-linking; *in vivo*.

Paper 190171RR received May 26, 2019; accepted for publication Sep. 6, 2019; published online Oct. 11, 2019.

## 1 Introduction

Riboflavin and UV-induced corneal collagen crosslinking (CXL) has been well-recognized as an effective treatment for progressive keratoconus.<sup>1</sup> The main step of CXL is a photochemical reaction between the riboflavin photosensitizer and UV light. This reaction strengthens the biomechanical properties of the cornea by increasing the covalent bonding in the stroma.<sup>2</sup> The widely used standard Dresden solution requires a 30-min infiltration of riboflavin solutions followed by 30 min of UV irradiation (3 mW/cm<sup>2</sup>, 5.4 J/cm<sup>2</sup>).<sup>3</sup> However, it is difficult for some patients, for example, children and patients with Down syndrome (a disease highly associated with keratoconus),<sup>4</sup> to keep themselves focused on the target over a 30-min treatment. According to the Bunsen–Roscoe law, the same effect can be achieved theoretically with an equal radiant energy provided by less intense UV radiation over a longer period of time or a more intense UV radiation over a shorter period of time.<sup>5</sup> This means the time of treatment could be shortened by increasing the irradiance within a safe range. However, several *in vitro* studies have found a decrease in the efficacy of accelerated CXL treatments due to oxygen depletion in the photochemical reaction. Although accelerated CXL treatments have shown promise in the clinic, an appropriate evaluation technique is necessary to find the balance between the time-consumption of CXL procedures and the efficiency.

There are several techniques available to evaluate the biomechanical properties of the cornea, such as uniaxial testing of corneal tissue strips and the inflation tests of entire cornea.<sup>5,6</sup> But these techniques cannot be applied *in vivo* samples, and conclusions from *in vitro* samples are fundamentally infeasible for *in vivo* applications. The ocular response analyzer and the Corvis ST (both from Oculus Inc., Arlington, Washington) are two commonly used devices in the clinic that can detect corneal

deformation in response to a high-volume air puff.<sup>6,7</sup> However, Young's modulus cannot be obtained from the results of the two approaches, and each has low spatial resolution caused by the wide area of deformation in response to the air puff and the change in intraocular pressure (IOP) induced by the large-amplitude deformation during the measurement. There is conflicting evidence in the literature on the ability of these devices to evaluate the effects of crosslinking on corneal biomechanical properties.<sup>8–10</sup>

Optical coherence tomography (OCT)-based elastography (OCE) is a rapidly emerging technique for noninvasively detecting biomechanical properties of ocular tissues.<sup>11</sup> Elasticity is measured by mechanical compression,<sup>12,13</sup> mechanical waves,<sup>14–17</sup> or resonance frequency<sup>18–20</sup> for OCE system. Various excitation systems, such as physical actuator,<sup>14</sup> air puff,<sup>15</sup> acoustic radiation force,<sup>16</sup> and laser pulse,<sup>17</sup> have been widely investigated. Like all forms of OCT, OCE has a superior micrometer scale resolution and is, therefore, suitable for imaging subtle biomechanical changes of the cornea due to diseases and/or therapeutic interventions such as CXL. Several studies based on OCE have shown that CXL altered corneal mechanical properties.<sup>21–24</sup> However, some contact-type OCE systems are unlikely to be well-applied *in vivo* for patients. So most studies were based on *in vitro* samples with a well-controlled IOP, which limits the use of OCE in clinic. The variation of IOP under *in vivo* conditions may lead to a nonlinear response of cornea and make the biomechanical properties difficult to be compared.<sup>25</sup>

This study proposed the use of a noncontact method of OCE with a microair puff excitation system to measure corneal biomechanical properties and evaluate the effect of CXL treatments with different irradiance strategies. A phase-stabilized swept light source OCT system was custom-built to detect low-amplitude elastic waves induced by focused air pulses onto the surface of rabbit corneas *in vivo* before and after CXL cross-linking. Young's modulus, a measure of corneal elasticity, was

\*Address all correspondence to Dexi Zhu, E-mail: zhudexiao@hotmail.com

calculated based on the group velocity of the elastic waves. To reduce the influence of the IOP variations on the measurement of Young's modulus, we constructed a curve based on data from whole eyes *in vitro* that compensated for the effect of different IOPs *in vivo*. This IOP-compensated OCE system was employed to compare the post-CXL corneal elasticity in response to different UV irradiance protocols.

## 2 Methods

### 2.1 OCE Experimental Setup

The OCE system comprised a custom-built swept-source OCT system and a microair-puff excitement system [Fig. 1(a)].

The broadband swept source laser (Axsun Technologies Inc., Billerica, Massachusetts) featured a center wavelength of 1050 nm with a bandwidth of 100 nm and a scan rate of 100 kHz. The output laser was divided by a fiber coupler, with 80% of the light going to the sample arm and 20% going to a static reference mirror. The returning light from both arms passed through fiber circulators and then recombined through a 50/50 optical coupler and detected by a high-speed balanced photodetector. The interference signal was then processed, and the depth information was extracted for each sampling point, including the structure and phase portions. Images of the cornea

were obtained with an axial resolution of 6  $\mu\text{m}$  and imaging depth of 3.8 mm in tissue.

The elastic wave was generated in the cornea by shooting a short duration ( $\leq 1$  ms) air-puff. Air-puff is the relatively ideal stimulating way on the cornea and has been applied in the existing medical equipment such as ORA and Corvis ST. The microair-puff system in our research was composed of a function generator, a solenoid valve controller, and a microair-puff nozzle. The pressure of the air, delivered at the limbus, was controlled by a high-precision relief valve from an air tank. The high-speed operation frequency of the solenoid valve (1200 Hz) and the small inner diameter of the nozzle (100  $\mu\text{m}$ ) resulted in a short stimulation time by the air puff on the cornea surface, covering a circular area 150 to 300  $\mu\text{m}$  in diameter. For safety considerations, the edge of the nozzle was designed to be flat and positioned precisely via a three-dimensional micromanipulator [Fig. 1(c)].

### 2.2 OCE Data Acquisition and Processing

During the acquisition, a trigger signal from a computer activated the microair-puff system and induced an elastic wave on the cornea. The OCT was set in M-mode, and the galvanometer was synchronized with the air-puff system by the same trigger

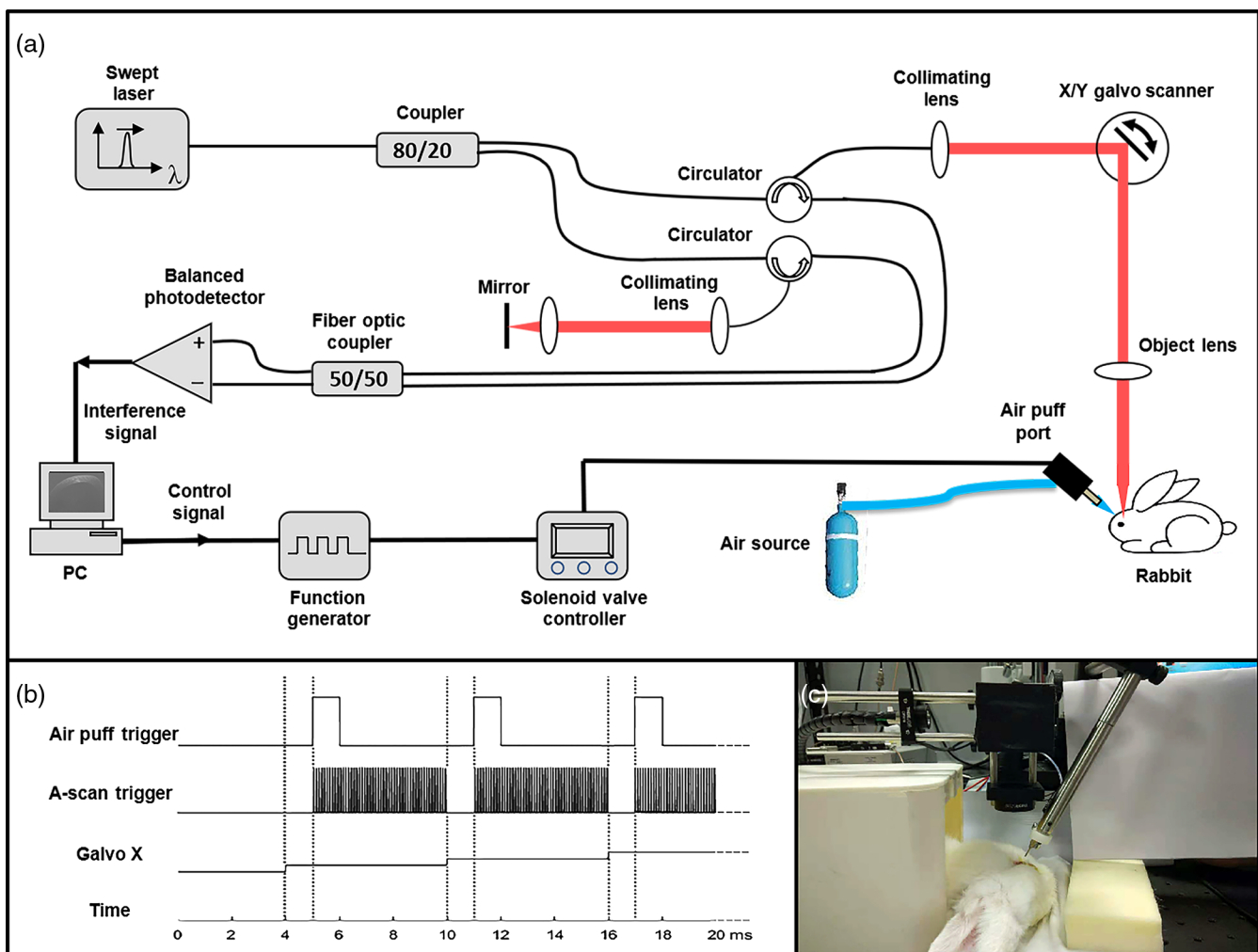


**Fig. 1** OCE system organization: (a) schematic diagram of the OCE experimental setup, (b) timing diagram of the OCE experimental setup, and (c) inset of the probe with experimental rabbit.

[Fig. 1(b)]. In this study, 50 position points ranging from the nasal limbus to the center of cornea were imaged. The distance between adjacent position point was set to be  $\Delta d = 120 \mu\text{m}$ . At each position, 500 A-lines were acquired continuously with a duration of 5 ms, which was enough for the OCT system to capture the elastic wave that propagated through each position (Fig. 2). The phase shift of the cornea was abstracted from the OCT signal based on the PRCD (phase-resolved color doppler) algorithm.<sup>21</sup> Therefore, the phase information at each position points was detected (Fig. 2). Then the time delay of the phase information between adjacent position points  $\Delta t$  was calculated by subtraction of the peak. The velocity of elastic wave between each adjacent position points  $c_g$  equals to  $\Delta d$  over  $\Delta t$ . Finally, Young's modulus  $E$  was quantified by<sup>22-24</sup>

$$E = \frac{2 \rho (1 + \nu)^3}{(0.87 + 1.12 \nu)^2} c_g^2, \quad (1)$$

where  $\nu = 0.49$  is the Poisson's ratio,<sup>26</sup>  $\rho$  is the density of cornea ( $\rho = 1.062 \text{ g/cm}^3$  for the cornea), and  $c_g$  is the group velocity of the elastic wave. This equation assumes that the excited elastic wave propagates as a Rayleigh wave model for elastic layers with semi-infinite thickness. It has been reported that the modified Lamb wave model is more suitable for cornea,<sup>27,28</sup> whose thickness is smaller than the characteristic wavelength. However, the change in the group velocity may still reasonably correspond to relative variations in the Young modulus, even though the absolute value may be not consistent.<sup>23</sup> Rayleigh wave model base on group velocity is also more accessible in clinical application.

OCE measurements were first performed on the agar samples with three concentrations (0.5%, 1%, and 2%) to evaluate the accuracy of the OCE system, and elastic wave velocity of the agar samples we got was compared with the reported data, as shown in Fig. 3.<sup>14</sup> The elastic wave velocity measured in our research tends to be a little smaller than the literature values, but it shows good stability overall.

### 2.3 Animals Experiments

Nine male white Japanese rabbits (2.5 to 3.5 kg, aged 3 to 4 months) were acquired from the Animal Breeding Unit of

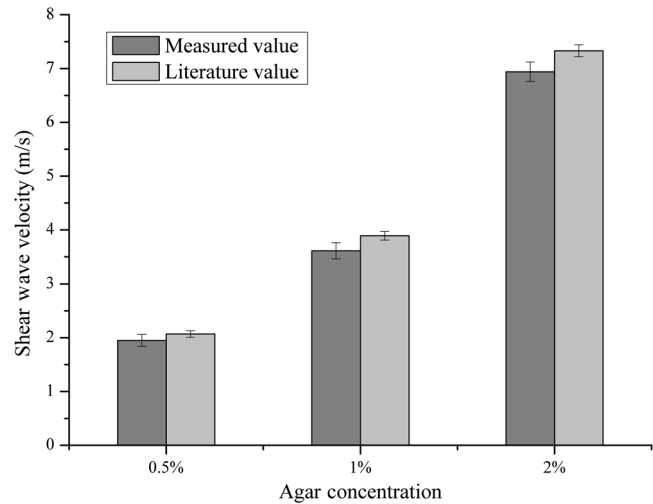


**Fig. 3** Elastic wave velocity of the agar samples with concentrations of 0.5%, 1%, and 2%.

Wenzhou Medical University and randomly assigned into three groups. Each group ( $n = 3$  rabbits) was assigned to a different irradiation protocol:  $3 \text{ mW/cm}^2$  for 30 min,  $9 \text{ mW/cm}^2$  for 10 min, or  $18 \text{ mW/cm}^2$  for 5 min. All rabbits were treated in accordance with the Association for Research in Vision and Ophthalmology Statement for Use of Animals in Ophthalmic and Vision Research and with the approval of the Animal Care and Ethics Committee of the Eye Hospital, Wenzhou Medical University. The sample size was calculated by a software program (Gpower, Ver. 3.1.9).<sup>29,30</sup> Three samples per group would be enough to detect the percentage change in elasticity between each group with the detection power of 0.95.

Three OCE measurements were performed on the left eye of each rabbit. The first OCE measurement was taken at baseline before any treatments. Then the rabbits were anesthetized with an intramuscular injection of pentobarbital sodium ( $30 \text{ mg/kg}$ ). A blepharostat was placed to hold the eyelids of each rabbit before the epithelium was removed by a hockey knife. Next, the cornea was infiltrated with 0.22% riboflavin solution (VibeX Xtra; Avedro, Inc., Waltham, Massachusetts) for 30 min. The CXL treatment was then performed via an ultraviolet

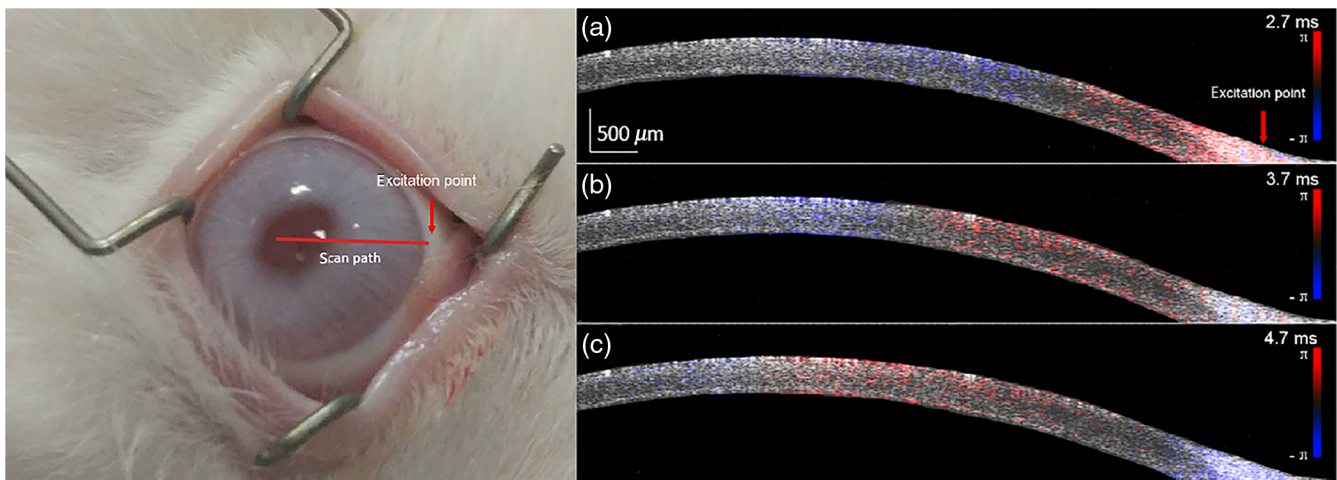


**Fig. 2** Phase shift during propagation of the elastic wave: (a) phase shift at 2.7 ms after the trigger, (b) phase shift at 3.7 ms after the trigger, and (c) phase shift at 4.7 ms after the trigger.

radiation A (UVA) irradiation system (CL-01; SiHaiTong Co., Suzhou, China) with one of the three irradiation protocols described above.<sup>31</sup> The second OCE measurement was taken immediately after the CXL treatment. The third OCE measurement was performed at one week after the CXL treatment. All OCE measurements were repeated for three times. The mean Young's modulus was measured from the average group velocity on the central cornea within a range of 4 mm. The group velocity is estimated by applying a linear regression to the phase displacement map with the time shifts versus the propagating distance laterally. The IOP was monitored through an ophthalmic tonometer (Tono-Pen; AVIA, Reichert Technologies, Depew, New York) during the three OCE measurements. All rabbits received tobramycin ophthalmic drops three times per day during the recovery process to prevent bacterial infections.

IOP has a documented influence on the elastic modulus due to the nonlinear response of cornea.<sup>25</sup> IOP fluctuates at different times under *in vivo* conditions, so it is almost impossible to keep the IOP at the same level during the three OCE measurements. Therefore, comparing the biomechanical properties between the

pre- and postoperative periods required a uniform IOP for each of the measurements. In order to obtain the relationship between IOP and Young's modulus, after the last OCE data acquisition, each of the nine rabbits was killed by an injected overdose of pentobarbital sodium (100 mg/kg). Then both eyeballs were immediately removed for the OCE measurements at controlled IOPs ranging from 1 to 20 mmHg that was set by a custom-built IOP control device.<sup>32,33</sup> The data acquired from the measurements were used to create correction curves to adjust for the IOP when comparing the biomechanical properties. Several representative correction curves in each group were shown in Fig. 4

### 3 Results

Figure 5 shows the structure images of a specific cornea from the 9-mW/10-min group at three measurements. The central thickness of cornea increases after the CXL because of the edema, and one week later, the morphology of cornea recovers as the original state. The velocity maps of the elastic waves were calculated from the phase-shift delay and then converted to elastograms. The effect of IOP on the corneal stiffness was

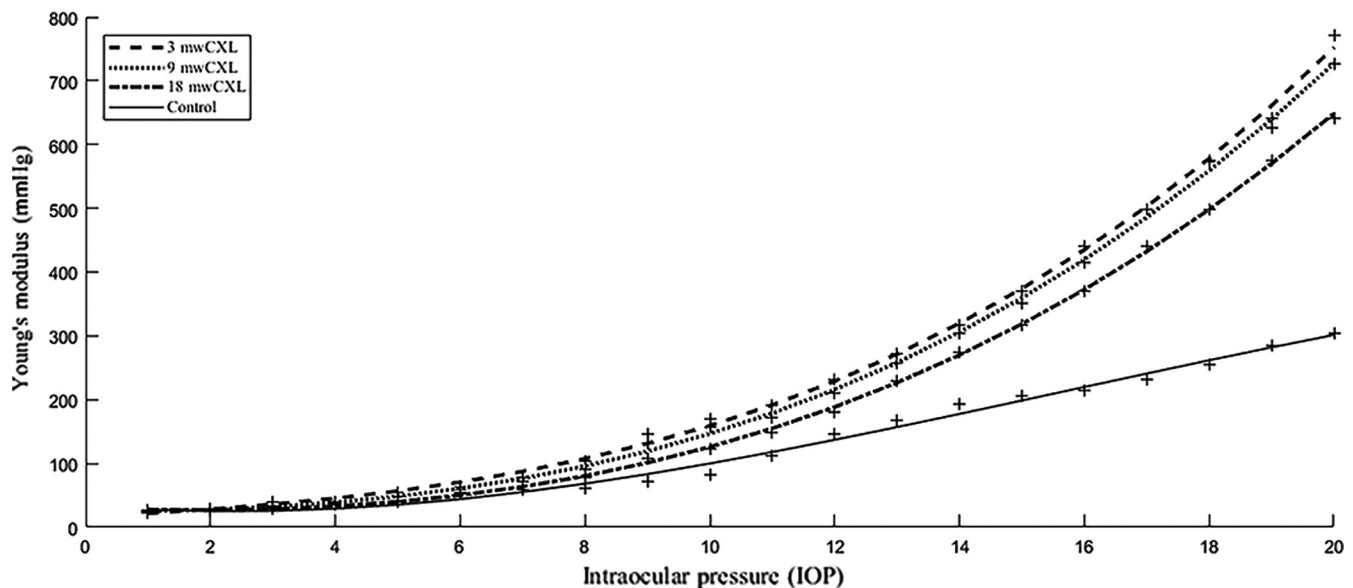


Fig. 4 Correction curves from IOP controlled OCE experiments.

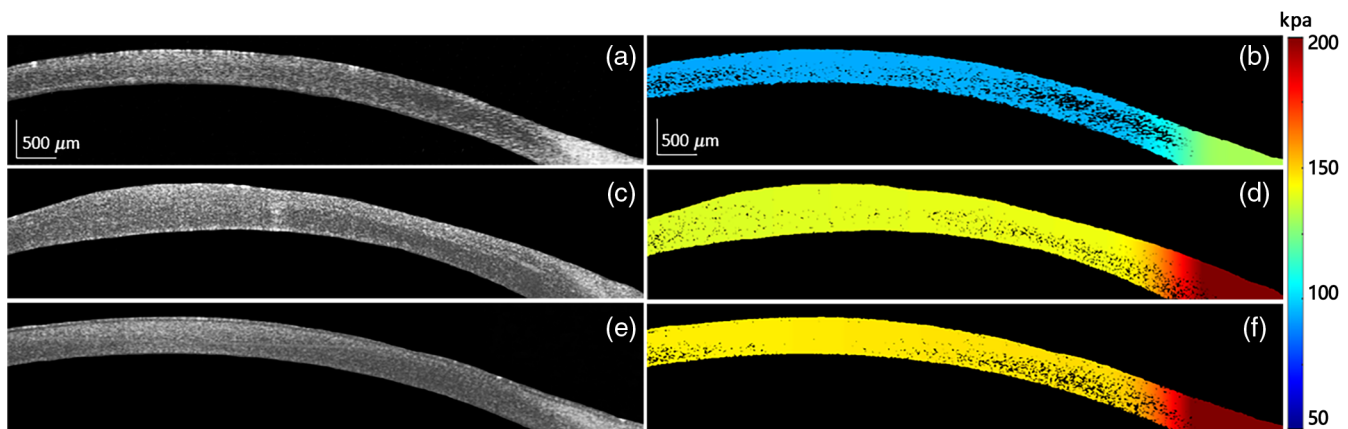
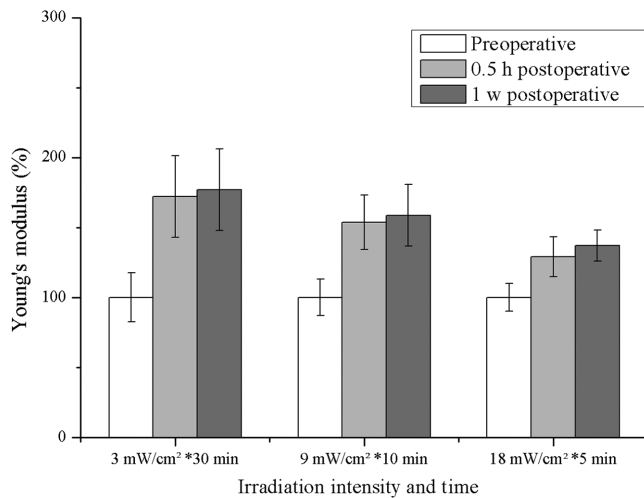


Fig. 5 Representative *in vivo* structure and elastogram images of a cornea from the 9-mW/10-min group: (a), (c), (e) rabbit corneal structure images at pre-, post- and one-week after operation, respectively, and (b), (d), (f) elastograms at pre-, post- and one-week after operation, respectively.



**Fig. 6** Effect of irradiation intensity and time on Young's modulus of cornea.

eliminated by adjusting at a uniform IOP of 11 mmHg according to the correcting curve shown in Fig. 4.

A clear distribution in elasticity from limbus to cornea was projected on the structure images, as shown in Fig. 5. Young's modulus clearly increases after the CXL treatment in all three groups. For one of the group 9 mW/10 min, the Young's modulus before the CXL treatment was  $131.1 \pm 7.4$  kPa at the limbus and decreases gradually from the limbus to the central cornea, where the Young's modulus was  $93.7 \pm 1.3$  kPa. After the CXL treatment, the modulus increased and was  $203.2 \pm 11.4$  kPa at the limbus and  $142.9 \pm 6.3$  kPa at the central cornea. After one week of recovery, the elasticity at the central cornea was  $147.7 \pm 5.5$  kPa, a slight increase over the value immediately after CXL treatment.

The normalized Young's modulus for the three treatment protocols at central cornea was compared in Fig. 6. If the Rayleigh approximation was valid, 100% values in each group correspond to 108.2, 106.4, and 121.9 kPa, respectively. The improvement in elasticity was more with lower irradiation over longer periods of time ( $p < 0.05$ ). For the 3-mW/30-min group, which was identical to the Dresden solution, the mean Young's modulus increased by 73.7% above the baseline after the CXL treatment. For the 9-mW/10-min group, it increased by 53.7%. Although for the 18-mW/5-min group, the increase was the smallest (32.9%). After one week of recovery, the modulus increases by a small amount for all groups, i.e., 3.8% for the 3-mW/30-min group, 3.2% for the 9-mW/10-min group, and 2.9% for the 18-mW/5-min group.

#### 4 Discussion

This study presented a noninvasive OCE system to construct *in vivo* elasticity maps of the cornea. OCT is a common resource in ophthalmic clinics, and the microair puff adopted in this OCE system is gentler than the existing medical equipment such as in the ORA and Corvis ST. This technology is potentially a practical method to observe the subtle changes in biomechanical properties of the cornea, which will be clinically helpful in the early diagnosis and treatment of corneal diseases.

To evaluate the practicability of this OCE system, we compared the biomechanical differences in rabbit corneas given different CXL protocols while keeping the total energy delivered constant. Corneas in the group receiving 3 mW/30 min UVA

showed the largest percent changes in Young's modulus after the CXL treatment. This indicates that the protocol adopted in that group has the best CXL effect. With increased irradiance delivered over shorter periods of time, as in the 9-mW/10-min and the 18-mW/5-min UVA groups, the effect of CXL on Young's modulus became weaker, similar to a previously reported study conducted *in vitro*.<sup>34</sup>

During the CXL reaction, oxygen is consumed and transformed into reactive oxygen species.<sup>35</sup> Hence, higher or lower oxygen partial pressure would cause an increase or decrease in the efficacy of CXL,<sup>36</sup> respectively. In the high UVA irradiance schemes such as the 9-mW/10-min and 18-mW/5-min groups, local oxygen consumption may surpass the oxygen provided by free diffusion in cornea, and in that case, the CXL effect would be reduced.<sup>35</sup>

The ability of noninvasive *in vivo* measurements enables the possibility of follow-up studies in clinical application. In this study, we measured variations of Young's modulus during the recovery process. As observed from the representative structure image in Fig. 5, the central thickness of the cornea restores from 595 to 465  $\mu$ m one week after the CXL treatment, and a subtle increase of Young's modulus was present in all groups. In general, the epithelium in all eyes recovers from wounds within 48 h,<sup>37</sup> and the dehydration of the stroma induced by the new epithelium increases the density of collagen fibers. In theory, these changes could slightly increase Young's modulus of the cornea.<sup>38</sup> To the best of our knowledge, this is the first time that the subtle increase in Young's modulus was verified *in vivo* for the recovered cornea after the CXL treatment.

Because IOP has a remarkable influence on the measurement of corneal stiffness,<sup>39</sup> the effects of different CXL protocols must be compared under the same IOP for each eye. However, it is impossible to control the IOP accurately and noninvasively in practice. In this study, the Young's modulus in enucleated whole rabbit eyes at IOPs ranging from 1 to 20 mmHg were measured *in vitro* using a closed-loop IOP control system. Based on these data, the measured values of modulus were corrected at a uniform IOP of 11 mmHg regardless of the actual IOP, in which the *in vivo* measurements were made. Based on this approach, the influence of IOP variations was almost eliminated during the comparison of the corneal biomechanical properties.

The major advantage of our *in vivo* measurement was the consideration of the factors in living organisms and cells. For example, the regulation of oxygen is a crucial factor in the CXL reaction. It is regarded as the primary bottleneck of the CXL reaction initiated with high UVA irradiance.<sup>40</sup> Physiological regulation provides an extra supplement of oxygen in the *in vivo* cornea and may increase the local oxygen partial pressure, making the process of CXL more efficient. Another important different between *in vivo* and *in vitro* cornea is the function of the corneal endothelium. The latter is a vulnerable and vital structure that keeps the cornea dehydrated. Once it is damaged, corneal elasticity would reduce due to edema.<sup>38</sup> Endothelium damage may be one of the reasons why elasticity measured in most *in vitro* experiments is generally lower than *in vivo*.<sup>28,31,32,41</sup> In sum, there is considerable inconsistency in the results of *in vitro* studies due to different conditions and specimens. The inconsistency of these outcomes makes it uncertain how much the CXL improving the stiffness of cornea. In contrast, *in vivo* conditions of the current study are relatively stable and more similar to the real clinic condition.

There are several limitations in our study. First, the air puff should be further decreased by improving the sensitivity of the OCT system in follow-up studies. Second, the curve fitting protocol to compensate for the effect of different IOPs on Young's modulus was generated from the corneas of whole rabbit eyes through *in vitro* experiments but cannot be applied to human eyes. IOP-fitting curves of human corneas can be acquired from human donor eyes or a large sample data set from clinical examinations. Finally, although the group velocity-based measurement can reasonably reflect the relative changes in the Young modulus, the modified Lamb wave model should be used if the absolute and precise value is required. Future research based on the modified Lamb wave model with big sample size will be performed to evaluate the effect of CXL in cornea.

## 5 Conclusions

This paper demonstrated a noninvasive method of producing *in vivo* the corneal elasticity map. The biomechanical differences in rabbit corneas with different CXL protocols were detected *in vivo*. The results indicate that the effect on Young's modulus was weaker when treated with higher irradiance levels over decreased durations, and a subtle increase of Young's modulus was present in all groups one week after the recovery process. Based on the noninvasive and *in vivo* measurement with the OCT and air-puff delivery system, this technique has great potential for the early detection and treatment of corneal diseases such as keratoconus and other related diseases.

## Disclosures

The authors declare that there are no conflicts of interest related to this article.

## Acknowledgments

The authors would like to thank Dr. Chenwei Wu for his help in several CXL operations in this study. This work was supported by the National Key Research and Development Program of China (Nos. 2016YFC0102500 and 2016YFE0107000); the National Nature Science Foundation of China (Grant No. 81570880); and the Natural Science Foundation of Zhejiang Province (Grant No. LY18H180008).

## References

- G. Wollensak, E. Spoerl, and T. Seiler, "Riboflavin/ultraviolet-a-induced collagen crosslinking for the treatment of keratoconus," *Am. J. Ophthalmol.* **135**(5), 620–627 (2003).
- G. Wollensak, E. Spoerl, and T. Seiler, "Stress-strain measurements of human and porcine corneas after riboflavin-ultraviolet-A-induced cross-linking," *J. Cataract Refract. Surg.* **29**(9), 1780–1785 (2003).
- C. S. Medeiros et al., "Accelerated corneal collagen crosslinking: technique, efficacy, safety, and applications," *J. Cataract Refract. Surg.* **42**(12), 1826–1835 (2016).
- J. L. Alio et al., "Corneal morphologic characteristics in patients with down syndrome," *JAMA Ophthalmol.* **136**(9), 971 (2018).
- A. Schindl, B. Rosado-Schlosser, and F. Trautinger, "Reciprocity regulation in photobiology. An overview," *Hautarzt* **52**(9), 779–785 (2001).
- C. Tao et al., "Corneal hysteresis with intraocular pressure of a wide range: a test on porcine eyes," *J. Refract. Surg.* **29**(12), 850–854 (2013).
- Z. Han et al., "Air puff induced corneal vibrations: theoretical simulations and clinical observations," *J. Refract. Surg.* **30**(3), 208–213 (2014).
- S. Bak-Nielsen et al., "Dynamic Scheimpflug-based assessment of keratoconus and the effects of corneal cross-linking," *J. Refract. Surg.* **30**(6), 408–414 (2014).
- M. Gkika et al., "Evaluation of corneal hysteresis and corneal resistance factor after corneal cross-linking for keratoconus," *Graefes Arch. Clin. Exp. Ophthalmol.* **250**(4), 565–573 (2012).
- Y. Goldich et al., "Can we measure corneal biomechanical changes after collagen cross-linking in eyes with keratoconus?: a pilot study," *Cornea* **28**(5), 498–502 (2009).
- J. Fujimoto and E. Swanson, "The development, commercialization, and impact of optical coherence tomography," *Invest. Ophthalmol. Vis. Sci.* **57**(9), OCT1 (2016).
- V. Y. Zaitsev et al., "Revealing structural modifications in thermomechanical reshaping of collagenous tissues using optical coherence elastography," *J. Biophotonics* **12**, e201800250 (2018).
- A. A. Sovetsky et al., "Manually-operated compressional optical coherence elastography with effective aperiodic averaging: demonstrations for corneal and cartilaginous tissues," *Laser Phys. Lett.* **15**(8), 085602 (2018).
- S. Song et al., "Shear modulus imaging by direct visualization of propagating shear waves with phase-sensitive optical coherence tomography," *J. Biomed. Opt.* **18**(12), 121509 (2013).
- S. Wang and K. V. Larin, "Noncontact depth-resolved micro-scale optical coherence elastography of the cornea," *Biomed. Opt. Express* **5**(11), 3807 (2014).
- Y. Qu et al., "In vivo elasticity mapping of posterior ocular layers using acoustic radiation force optical coherence elastography," *Invest. Ophthalmol. Vis. Sci.* **59**(1), 455 (2018).
- S. Li et al., "Dual shear wave induced laser speckle contrast signal and the improvement in shear wave speed measurement," *Biomed. Opt. Express* **6**(6), 1954 (2015).
- A. Manduca et al., "Magnetic resonance elastography: non-invasive mapping of tissue elasticity," *Med. Image Anal.* **5**(4), 237–254 (2001).
- E. W. Chang, J. B. Kobler, and S. H. Yun, "Subnanometer optical coherence tomographic vibrography," *Opt. Lett.* **37**(17), 3678 (2012).
- B. I. Akca et al., "Observation of sound-induced corneal vibrational modes by optical coherence tomography," *Biomed. Opt. Express* **6**(9), 3313 (2015).
- G. Liu et al., "A comparison of Doppler optical coherence tomography methods," *Biomed. Opt. Express* **3**(10), 2669 (2012).
- B. F. Kennedy, K. M. Kennedy, and D. D. Sampson, "A review of optical coherence elastography: fundamentals, techniques and prospects," *IEEE J. Sel. Top. Quantum Electron.* **20**(2), 272–288 (2014).
- Z. Han et al., "Quantitative methods for reconstructing tissue biomechanical properties in optical coherence elastography: a comparison study," *Phys. Med. Biol.* **60**(9), 3531–3547 (2015).
- J. Li et al., "Dynamic optical coherence tomography measurements of elastic wave propagation in tissue-mimicking phantoms and mouse cornea *in vivo*," *J. Biomed. Opt.* **18**(12), 121503 (2013).
- D. A. Hoeltzel et al., "Strip extensimetry for comparison of the mechanical response of bovine, rabbit, and human corneas," *J. Biomech. Eng.* **114**(2), 202–215 (1992).
- Z. Han et al., "Analysis of the effects of curvature and thickness on elastic wave velocity in cornea-like structures by finite element modeling and optical coherence elastography," *Appl. Phys. Lett.* **106**(23), 233702 (2015).
- C.-C. Shih et al., "Quantitative assessment of thin-layer tissue viscoelastic properties using ultrasonic micro-elastography with Lamb wave model," *IEEE Trans. Med. Imaging* **37**(8), 1887–1898 (2018).
- Z. Han et al., "Optical coherence elastography assessment of corneal viscoelasticity with a modified Rayleigh-Lamb wave model," *J. Mech. Behav. Biomed. Mater.* **66**, 87–94 (2017).
- F. Faul et al., "G\*Power 3: a flexible statistical power analysis program for the social, behavioral, and biomedical sciences," *Behav. Res. Methods* **39**(2), 175–191 (2007).
- D. G. Bonett and T. A. Wright, "Sample size requirements for estimating Pearson, Kendall and Spearman correlations," *Psychometrika* **65**(1), 23–28 (2000).
- F. Bao et al., "Changes in corneal biomechanical properties with different corneal cross-linking irradiances," *J. Refract. Surg.* **34**(1), 51–58 (2018).
- M. Singh et al., "Noncontact elastic wave imaging optical coherence elastography for evaluating changes in corneal elasticity due to crosslinking," *IEEE J. Sel. Top. Quantum Electron.* **22**(3), 266–276 (2016).

33. C. Dorronsoro et al., "Dynamic OCT measurement of corneal deformation by an air puff in normal and cross-linked corneas," *Biomed. Opt. Express* **3**(3), 473 (2012).
34. A. Hammer et al., "Corneal biomechanical properties at different corneal cross-linking (CXL) irradiances," *Invest. Ophthalmol. Vis. Sci.* **55**(5), 2881 (2014).
35. P. Kamaev et al., "Photochemical kinetics of corneal cross-linking with riboflavin," *Invest. Ophthalmol. Vis. Sci.* **53**(4), 2360–2367 (2012).
36. S. Kling et al., "Increased biomechanical efficacy of corneal cross-linking in thin corneas due to higher oxygen availability," *J. Refract. Surg.* **31**(12), 840–846 (2015).
37. W. Abdel-Naby et al., "Treatment with solubilized Silk-Derived Protein (SDP) enhances rabbit corneal epithelial wound healing," *PLoS One* **12**(11), e0188154 (2017).
38. H. Hatami-Marbini and E. Etebu, "Hydration dependent biomechanical properties of the corneal stroma," *Exp. Eye Res.* **116**, 47-54 (2013).
39. T.-M. Nguyen et al., "In vivo evidence of porcine cornea anisotropy using supersonic shear wave imaging," *Invest. Ophthalmol. Vis. Sci.* **55**(11), 7545 (2014).
40. O. Richoz et al., "The biomechanical effect of corneal collagen cross-linking (CXL) with riboflavin and UV-A is oxygen dependent," *Transl. Vis. Sci. Technol.* **2**(7), 6 (2013).
41. X. Qian et al., "Ultrasonic microelastography to assess biomechanical properties of the cornea," *IEEE Trans. Biomed. Eng.* **66**(3), 647–655 (2019).

Biographies of the authors are not available.